A Simplified Model for Light Interaction with Plant Tissue

Gladimir V. G. Baranoski Jon G. Rokne

Department of Computer Science, The University of Calgary, Calgary, AB, Canada

Abstract

Rendering techniques currently used in computer graphics enable the generation of very realistic images of a wide range of materials. Despite of the latest achievements in this field, there are still areas, such as biological imaging, open for further investigation. In this paper a simplified model for light interaction with plant tissues is presented. It accounts for the main biological characteristics of these materials needed to preserve their rendering quality, while avoiding undue complexity in order to increase their rendering efficiency. The model's design and formulation are based on Monte Carlo techniques, and it can be incorporated into global illumination systems without a significant computational overhead. Its accuracy and performance are examined through comparisons with a biologically-based model whose spectral readings have been verified against experimental data for real specimens.

Keywords: *biologically-based rendering, reflectance, transmittance, bidirectional surface-scattering distribution function, scattering probability function.*

1 Introduction

The accuracy of simulations of light interaction with plants depends on the reflectance and transmittance models for foliar tissues. The use of physically-based models can ensure that the applied rendering methods do not violate the laws of physics [18]. Moreover, these models have to be biologically-based in order to appropriately account for the natural processes involved in these simulations. Simplicity is also an important requirement for a reflectance model, since, as pointed out by Ward [30], a model may otherwise become computationally impractical. Thus, it is necessary to design practical reflectance and transmittance models that allow us to render these materials fast without undermining the image quality.

Researchers from remote sensing and biology areas have proposed reflectance and transmittance models for plant leaves that relate their optical properties to their biological and biochemical characteristics [7, 13, 20, 28], but these models are not suitable for image synthesis applications. Reflectance models specifically oriented to these applications are, however, usually designed for a wide range of materials, and tend to overlook important biological factors which affect light propagation. Furthermore, the models oriented to the rendering of organic materials, like the multilayer model [12], have the drawback of relying on spectral curves of reflectance and transmittance which are only available in the literature for a few illuminating and viewing angles.

Recently a reflectance and transmittance model for plant tissue, the algorithmic BDF[1] model [2] (ABM, for short), was proposed to overcome these limitations. It computes the reflectances and transmittances through the incorporation of biological factors that affect light interaction with foliar tissues. Among these factors are the absorption curves of the pigments present in such tissues. The algorithmic nature of the ABM enables its easy incorporation into most rendering systems, but it makes its in-line application computationally expensive.

In this paper we present a simplified model for light interaction with plant tissues, which aims to provide a balance between two apparently conflicting goals, namely accuracy and efficiency. This model accounts for the three components of plant tissues' BDF (surface reflectance, subsurface reflectance and transmittance), and uses pre-computed reflectances and transmittances as scale factors in a stochastic simulation of the scattering profile of the foliar tissues. The use of these scale factors replaces the time consuming random walk process used by ABM to simulate the randomization and the absorption of light within the foliar tissues. Moreover, this approach reduces the number of rays needed to achieve a desired accuracy level in the results.

These factors are computed off-line using the ABM, since the spectral curves provided by this model have already been compared with experimental data of real foliar specimens, showing a high degree of accuracy [2]. Although the proposed simplified model is oriented to leaves, the most important plant surface interacting with light, it can easily be extended to other plant surfaces like petals and stems since they present similar optical and structural characteristics [5, 15]. We compare the results obtained using the proposed model with results obtained applying the ABM in-line.

The remainder of this paper is organized as follows. The next section presents background information relevant to this investigation. Section 3 describes the proposed model. Section 4 describes the testing parameters and procedures. Section 5 discusses the results and performance issues. The paper closes with a summary and directions for future research.

[1] *Bidirectional surface-scattering distribution function* (BSSDF or simply BDF [6]).

2 Background

2.1 Reflectance and Transmittance Terms

The fraction of light at wavelength λ incident from a direction ψ_i at a point x that is neither absorbed into nor transmitted through a given surface is called the absolute reflectance, $R(x, \psi_i, \lambda)$, of the surface. Similarly, the fraction of light transmitted through the surface is called the absolute transmittance, $T(x, \psi_i, \lambda)$. However, the reflectance and the transmittance do not describe the distribution of the reflected and transmitted light. The *bidirectional reflection distribution function* (BRDF) and the *bidirectional transmission distribution function* (BTDF) are used to overcome this limitation. As suggested by Glassner [6], they can be combined into the BDF, which can be expressed in terms of the ratio between the radiance of the surface seen from a point in a direction ψ and the incident power per unit of area.

However, as pointed out by Shirley [26], sometimes it is more convenient to work with the radiant power than with the radiance. Under these circumstances it is more natural to describe the surface reflection and transmission properties in terms of the probability distribution of the reflected and transmitted light. This term can be called *scattering probability function* (SPF) [26]. It describes the amount of energy scattered in each direction ψ as:

$$s(x, \psi_i, \psi, \lambda) = \frac{dI(x, \psi, \lambda)}{R(x, \psi_i, \lambda) d\Phi(x, \psi, \lambda)} \qquad (1)$$

where:

x = point of incidence.
ψ = direction of propagation.
dI = radiant intensity scattered in the direction ψ.
$d\Phi$ = radiant power incident from ψ_i at x.

The term $R(x, \psi_i, \lambda)$ appears in the numerator when we are dealing with the reflection of light. It scales the function to a valid probability density function (PDF) [11] over the solid angle through which the reflected light leaves the surface. In the case of the transmission of light, a similar expression is used, in which $R(x, \psi_i, \lambda)$ is replaced by $T(x, \psi_i, \lambda)$.

2.2 Interaction of Light with Foliar Tissues

A leaf can be described as a diffusing and pigmented structure (mesophyll) having external plates of epidermal cells with a protective wax layer (cuticle). The surface roughness characteristics and the refraction index of the cuticle control the specularly reflected light from the adaxial (front) and abaxial (back) epidermis. The mesophyll contains pigments whose concentration and distribution control the absorption of light in the visible region of the light spectrum within a leaf.

Grant et al. [8] describe leaves as having both specular and diffuse characteristics. The specular (non-Lambertian) character of the leaf reflectance arises at the surface of the leaf. For some viewing directions, the surface reflectance may be so large that the leaves appear to have the color of the light source instead of green (Figure 1). This happens when the reflected light visually overwhelms the much smaller amounts of green light scattered by the interior of the leaves. The diffuse (Lambertian) character of leaf's reflectance emanates primarily from the mesophyll tissue through multiple scattering, with a small contribution of scattering from rough elements on the leaf surface. The multiple scattering in the leaf's interior also gives the leaf's transmittance a near-Lambertian distribution.

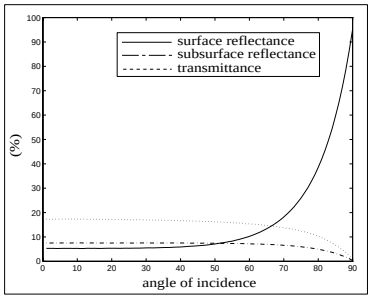

Figure 1: Curves of reflectance and transmittance of a soybean leaf obtained using the ABM [2] at a wavelength of $550nm$ and considering the leaf's front (adaxial epidermis) towards the light source.

2.3 Overview of the Algorithmic BDF Model

In the ABM [2] light propagation is described in terms of ray optics, where light is assumed to be composed of non-interacting straight rays, each of them carrying a certain amount of energy [9]. Instead of geometrically modeling many cells individually [7], the propagation of light within the foliar tissues is simulated as a stochastic process whose states are associated with the air-cell wall interfaces. Once a ray enters the leaf it can be reflected or refracted multiple times until it is either absorbed or propagated back to the environment.

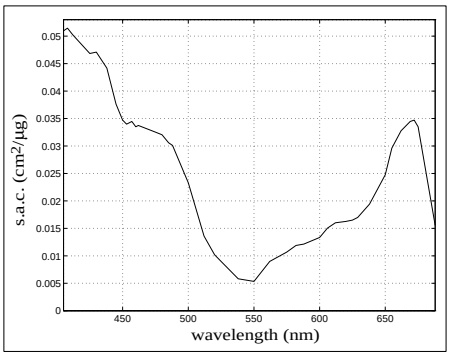

Figure 2: Curve for specific absorption coefficient (s.a.c.) of chlorophyll used by the ABM (adapted from [13]).

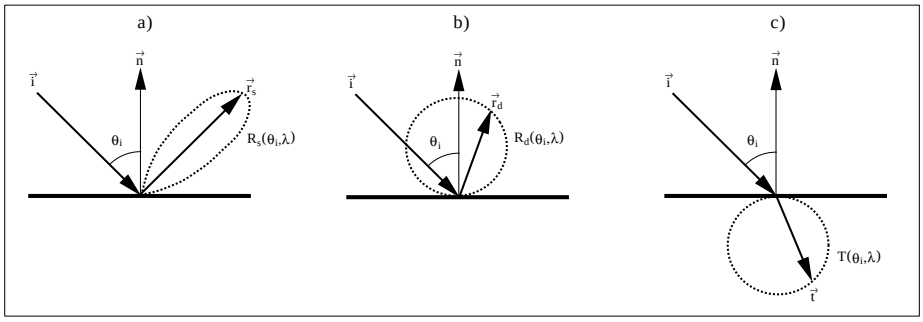

Figure 3: Scattering distribution performed by the simplified model to represent the three components of a foliar specimen's SPF: a) surface reflectance b) subsurface reflectance and c) transmittance.

The absorption testing executed by the ABM assumes a homogeneous distribution of pigments, and it is performed probabilistically every time a ray starts a run in the mesophyll tissue. It consists of the estimation of the ray free path length, p, using an expression based on Beer's law [1, 21]. If p is greater than the thickness of the pigmented medium, then the ray is propagated, otherwise it is absorbed. In order to compute p, it is necessary to sample the curves for the specific absorption coefficients of the pigments presented in this tissue, such as chlorophyll (Figure 2). The number and spacing between sample points will depend on the strategy used to guide the selection of wavelengths for image generation.

3 The Simplified Model

In the simplified model light propagation is also described in terms of ray optics, and the interaction of light with the foliar tissues is described in terms of their SPF. As pointed out by Glassner [6], the BDF (or, in our case, the SPF) is a difficult function to work with due to its dependence on several variables. Fortunately, we can make some simplifying assumptions about the foliar tissues that give us a more computationally convenient expression to manipulate.

First, we assume that the physical properties describing the light propagation are identical everywhere within the foliar tissues, i.e. they can be considered as homogeneous interacting media [7]. This assumption allows us to leave out the positional argument. Second, since the anisotropy of plant leaves is considered to be associated with their venation system [31], and considering that the biological data regarding these systems is scarce to support the design of a biologically-based anisotropic reflectance model for these materials, we also assume that they are isotropic. This assumption allows us to work with only one parameter for the direction ψ_i, which is given by the angle of incidence, θ_i, of an incident ray with respect to the normal of a leaf.

The proposed model takes into account the three components of the SPF of a plant tissue, namely surface reflectance, subsurface reflectance and transmittance. The contribution from each of these components is scaled using the respective values of absolute reflectance ($R_s(\theta_i, \lambda)$ and $R_d(\theta_i, \lambda)$) and absolute transmittance ($T(\theta_i, \lambda)$), as sketched in Figure 3. These are computed off-line using the ABM [2] and stored in a table.

The parameter space of the foliar SPF is represented by the input directional parameter space and the output directional parameter space. The first is given by the angle of incidence θ_i ($[0, \pi]$), and the second is given by the azimuthal angle θ ($[0, 2\pi]$) and the polar angle ϕ ($[0, \pi]$). The domain chosen for θ_i accounts for differences in the reflectance and transmittance curves of foliar specimens that differ markedly in the structure of their two sides. For specimens that do not present this characteristic [29] or for applications that assume identical optical properties for both sides [23], the domain of θ_i can be narrowed to $[0, \frac{\pi}{2}]$.

3.1 Surface Reflectance

When a ray hits the epidermis of a foliar specimen it may be propagated to internal tissues or be reflected back to the environment. Brakke et al. [3] have noted that the scattering profile of a plant leaf can be approximated by an exponentiated cosine function. In the simplified model a similar approach is used to simulate the distribution of the rays reflected at the foliar tissues. Govaerts et al. [7] have shown that the epidermal cells can be approximated by oblate ellipsoids which have semi-axes a_1, a_2 and a_3, with $a_1 = a_2$ and $a_1 > a_3$ [27]. For the plant cells we consider a_1 and a_2 as the axes in the plane of the foliar tissues, with values corresponding to average radius, a_r, of the cell. We define the oblateness of the cell as $\frac{a_r}{a_3}$. Based on the epidermal cells' dimensions for several species of plants found in the literature [7, 22], an appropriate range for the oblateness would be [0.2,5].

Initially, to account for the surface component of a foliar specimen's SPF for a given incident ray, we obtain the corresponding reflected ray using the law of reflection (angle of incidence, θ_i, equal to the angle of reflection, θ_r). Then, to simulate the effects of the epidermal cells' shape on the reflected rays at the air→epidermal cells interface, we perturb the reflected rays using a warping function (2). This function corresponds to a PDF based on an exponentiated cosine distribution [16], and the exponent is given by the oblateness of

the epidermal cells. The perturbation is performed through angular displacements, α_e and β_e. The angle α_e corresponds to the polar angle with respect to the ideal reflection or ideal transmission direction. The angle β_e corresponds to the azimuthal angle around the ideal reflection or ideal transmission direction. These angles are given by:

$$(\alpha_e, \beta_e) = (\arccos[(1-\xi_1)^{\frac{1}{ob+1}}], 2\pi\xi_2) \qquad (2)$$

where:
ξ_1 and ξ_2 = uniform random numbers $\in [0,1]$.
ob = oblateness of the epidermal cells.
Therefore leaves whose epidermal cells' oblateness is large will have a surface reflectance closer to a specular distribution than leaves whose epidermal cells' oblateness is small.

3.2 Subsurface Reflectance and Transmittance

When light passes to the internal tissues its direction of travel is randomized and it becomes diffuse. This randomization of the incident rays results in a near-Lambertian distribution for the subsurface reflectance of a foliar specimen, and a near-Lambertian distribution for its transmittance. In order to simulate the distribution of rays regarding these two components, we perturb the normal of the foliar specimen instead of the incident ray. The orientation of the normal used in the perturbation depends on the incidence geometry. If the incident ray hits the foliar specimen's front (adaxial epidermis) we use the normal for the subsurface reflectance component and its opposite vector for the transmittance component. Otherwise, we use the normal and its opposite vector the other way around.

For these perturbations we use another warping function(3), whose PDF corresponds to a diffuse or cosine distribution [16]. The perturbation is also performed through angular displacements, α_m and β_m. The angle α_m corresponds to the polar angle with respect to the reflection or transmission direction of the propagated ray. The angle β_m corresponds to the azimuthal angle around the propagation direction. These angles are given by:

$$(\alpha_m, \beta_m) = (\arccos(\sqrt{\xi}_1), 2\pi\xi_2) \qquad (3)$$

where:
ξ_1 and ξ_2 = uniform random numbers $\in [0,1]$.

4 Testing Parameters and Procedures

For our experiments we selected, without loss of generality, foliar data regarding a soybean leaf [2]. The absolute reflectance and transmittance measurements were made using a virtual spectrophotometer [2] and 10^6 rays in regular intervals of 1° for the angle of incidence θ_i ($[0,\pi]$). The comparisons regarding the foliar specimen's BDF presented in the next section were performed using a virtual goniophotometer [2] with a collector sphere divided into 20 patches along its latitude and 40 patches along its longitude and 10^8 rays per curve. As pointed out by Lalonde and Fournier [17], the use of these virtual devices give us control over the data generation and allow us to avoid measurement errors.

Lilley et. al [19] mention that to provide the correct colour in high quality computer graphics, the CIE XYZ values should be converted to the RGB colour space of a monitor using the SMPTE[2] monitor chromacity coordinates. In fact, many monitors used in the current workstations use these coordinates. Thus, we decided to sample the absorption curve for chlorophyll (Figure 2) in the dominant wavelengths corresponding to these coordinates (Table 1) in order to generate the table of reflectances and transmittances. Note that the dominant wavelength regarding the green channel corresponds to the wavelength for which the absorption of light by chlorophyll is minimum.

Table 1: Chromacity coordinates and wavelength values.

	x	y	wavelength
Red	0.630	0.340	$608nm$
Green	0.310	0.595	$551nm$
Blue	0.155	0.070	$455nm$
white (D65)	0.313	0.329	

The images presented in the next section were generated using a modified version of Kajiya's path tracing [14, 26]. For the computation of the direct light contribution we selected the scale factors $R_d(\theta_i, \lambda)$ and $T(\theta_i, \lambda)$ according to the position of the light source with respect to the foliar specimen. This selection was made using the angle of the shadow ray with respect to the specimen's normal, θ_s, and applying the following criteria:

$$- \text{ for } 0^\circ < \theta_s \leq 90^\circ \begin{cases} \frac{R_d(\theta_i,\lambda)}{\pi} & \text{if } 0^\circ < \theta_i \leq 90^\circ \\ \frac{T(\theta_i,\lambda)}{\pi} & \text{if } 90^\circ < \theta_i < 180^\circ \end{cases}$$

$$- \text{ for } 90^\circ < \theta_s < 180^\circ \begin{cases} \frac{T(\theta_i,\lambda)}{\pi} & \text{if } 0^\circ < \theta_i \leq 90^\circ \\ \frac{R_d(\theta_i,\lambda)}{\pi} & \text{if } 90^\circ < \theta_i < 180^\circ \end{cases}$$

While the ABM uses an explicit mechanism to simulate the absorption of light, the simplified model relies on the absorption probabilities implicitly associated with the scaling factors. In order to perform fair comparisons between these two models, we use an adaptive tree-depth control [10] based on cumulative ray attenuation (attenuation, for short) in our implementation of the path tracing algorithm. The attenuation of a ray is obtained through the product of the reflectance and/or transmittance of the surfaces hit in the ray's path [26]. It is then compared with a cutoff attenuation threshold, ϵ, to control the depth of the tree during the ray-tracing. For a given scene we select a value for ϵ to make the process using

[2] Society of Motion Picture and Television Engineers.

the simplified model stop with the same ratio of unshot rays to the total number of shot rays (0.01%) as the process using the ABM. Since the attenuation has three values corresponding to the three RGB channels, we convert it to luminance in order to compare it with a selected ϵ (0.01). This conversion is made using the following SMPTE formula [19]:

$$Y = 0.21222\ R + 0.7013\ G + 0.0865\ B \qquad (4)$$

For a given graphics setting the measurements regarding both models were performed on the same machine. Moreover, the models were implemented using the same software guidelines to avoid differences that could affect the timing. The root-mean-square (RMS) errors [6] of the difference images, as presented in the next section, are computed from normalized pixel values (scaled to $[0, 1]$).

5 Results and Discussion

In order to perform a comprehensive evaluation of the BDF curves provided by the proposed model it would be necessary to consider all possible testing geometries. However, due to the large number of measurements needed, we limit our examination to selected representative cases. Figure 4 shows the BDF curves generated using the ABM and the simplified model, for angles of incidence of 30° and 45°, and considering the plane given by the direction of incidence and the specimen's normal. Notice that the curves provided by the simplified model capture the main characteristics of the foliar specimen's BDF, namely an angular dependency on the incident angle for the BRDF intermediate to that expected of diffuse and specular reflectors and a near-Lambertian distribution for the BTDF. They also present a good qualitative agreement with the curves provided by the ABM which agree with the experimental curves published by Breece and Holmes [4] and Wooley [31]. The small discrepancies are mainly related to the simplified nature of the proposed model, and do not significantly affect the image quality as we can see in Figures 5, 6 and 7.

Figures 5a and 5b shows the first set of images with front lit leaves. The curves presented in Figure 8 shows that for this graphics setting the rendering process using the simplified model converges faster, in terms of the ray-tracing tree-depth, than the rendering process using the ABM. In the second set (Figures 6a and 6b), the leaves are back lit. For this graphics setting we can also observe a faster convergence for the rendering process using the simplified model (Figure 9). In the third set (Figures 7a and 7b), only ambient light is used, and there are no direct lighting calculations involved. As in the previous settings, the rendering process using the simplified model converges faster (Figure 10). However, for this graphics setting the curve regarding the simplified model is smoother than the corresponding curves for the previous settings due to the fact that there are no transmitted rays successively traversing two leaves back and forth, as opposed to the previous cases.

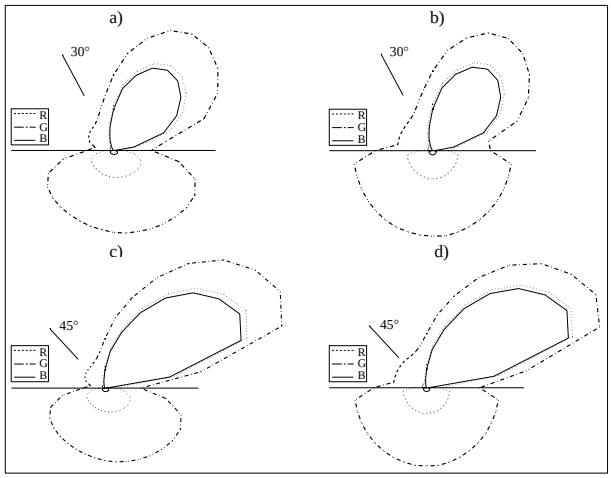

Figure 4: BDF curves obtained at the wavelengths associated with the RGB channels (Table 1) and considering the leaf's front (adaxial epidermis) towards the light source. a) and c) Using the ABM. b) and d) Using the simplified model. Curves for different angles of incidence present a similar agreement.

Although the convergence graphs (Figures 8, 9 and 10) are illustrative of the behavior of both models, they do not account for different types and amounts of work performed at each depth of the ray-tracing tree. In order to extend our performance evaluation, we have measured the speed up gains of the simplified model over the ABM for the three graphics settings. These speed up gains depend on a number of factors: the illuminating and viewing angles, the ratio of the number of pixels associated with the specimen(s) to the total number of pixels (in our case, called foliar ratio), the scene geometry, and the loss of quality threshold (in our case, given by the RMS errors). As mentioned earlier, the large number of measurements preclude us of looking at all these factors and their combinations at this point of our research. However, the figures presented in Table 2 suggest that the use of the simplified model can provide noticeable performance gains without a significant loss of image quality. This aspect in turn indicates that the simplified model is more suitable than the ABM for applications involving a large number of foliar primitives.

In order to reduce noise in the images due to Monte Carlo path tracing integration, we used a large number of sample points per pixel, which increased the absolute time measurements. For instance, the image presented in Figure 7b was generated using 400 sample points per pixel and it took 95 minutes (elapsed CPU time) on a SGI R10000. The incorporation of the model into more efficient global illumination frameworks may considerably reduce the overall rendering time.

The overhead of pre-computing the table of reflectances and transmittances is minimized by the fact that, for a given foliar specimen, this operation must be performed only once.

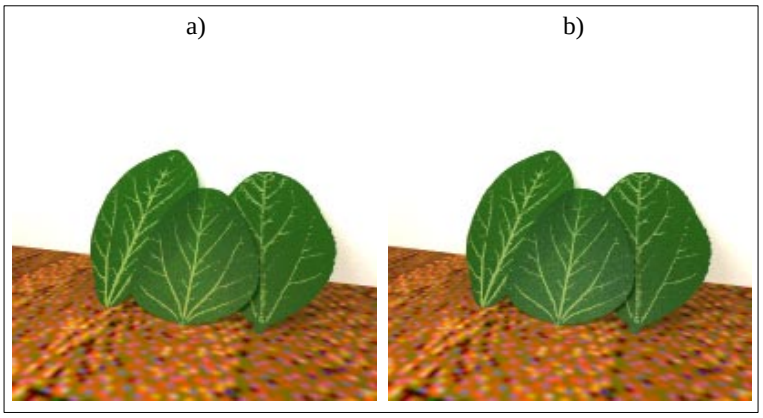

Figure 5: First set of images with the front (adaxial epidermis) of the leaves towards a light source. a) Using the ABM. b) Using the simplified model.

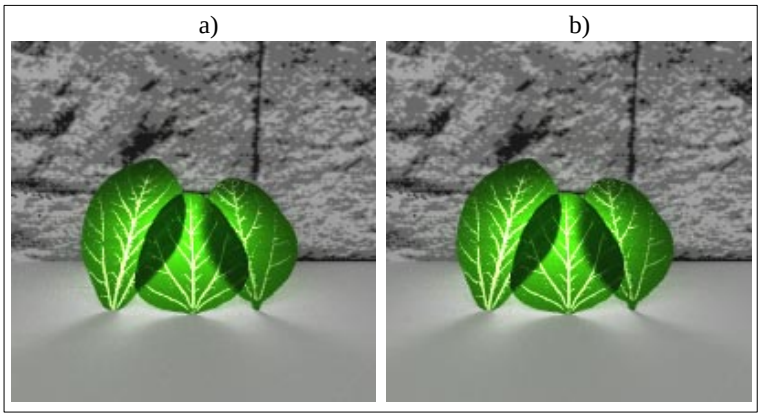

Figure 6: Second set of images with the back (abaxial epidermis) of the leaves towards the light source. a) Using the ABM. b) Using the simplified model.

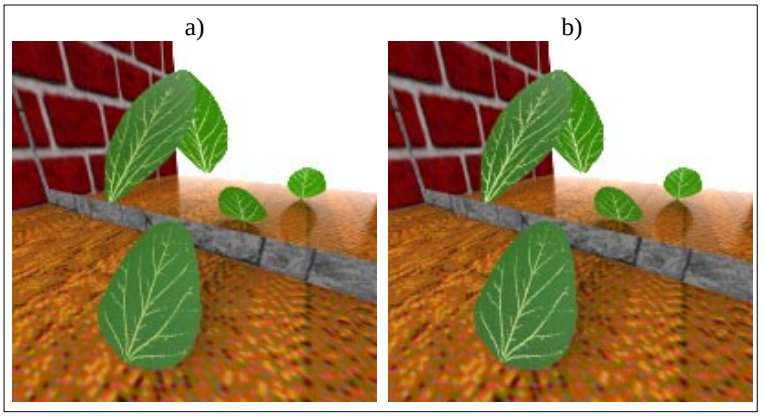

Figure 7: Third set of images with ambient light only. a) Using the ABM. b) Using the simplified model.

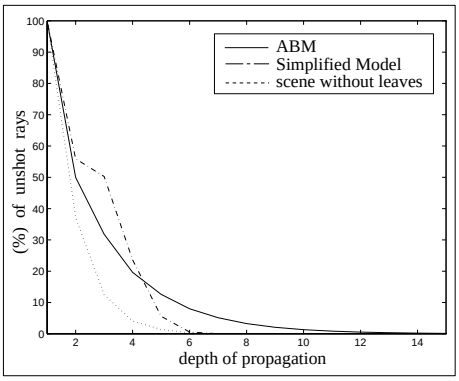

Figure 8: Convergence graph for the first set of images.

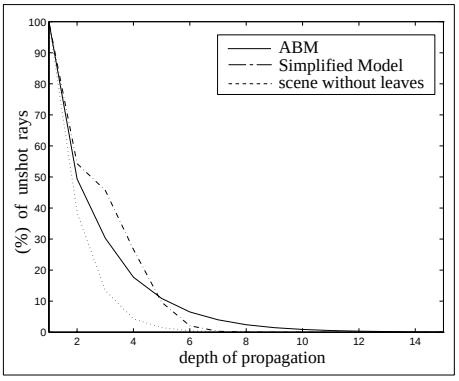

Figure 9: Convergence graph for the second set of images.

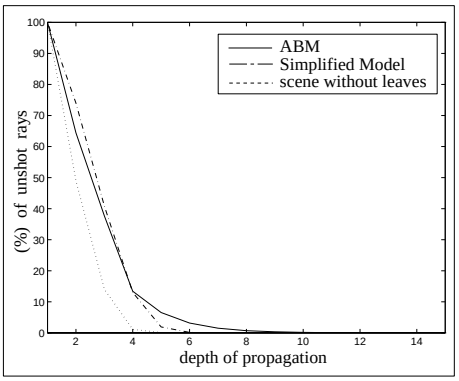

Figure 10: Convergence graph for the third set of images.

Table 2: Comparison of accuracy *vs.* performance gain.

set	foliar ratio	RMS error			speed up
		Red	Green	Blue	
1^{st}	24.97%	0.009	0.009	0.012	5.14
2^{nd}	19.42%	0.011	0.014	0.010	4.47
3^{rd}	37.61%	0.020	0.016	0.012	9.77

Then, the resulting table can be used several times not only in the rendering of individual leaves, but also in global illumination calculations involving vegetation canopies [23]. Furthermore, the table look-ups are performed through direct indexing and its storage requirements are within reasonable limits. For instance, the table used in our testing experiments requires only 14.5 Kb of storage space. Even if finer sampling resolutions are used in the measurement of reflectances and transmittances, we believe that the use of such a table provides a worthwhile trade-off between accuracy and computational costs, specially considering the sizes of the memories available nowadays and their decreasing costs.

6 Conclusion

We have presented a physically and biologically-based model for light interaction with plants that can be incorporated into rendering systems without a significant computational overhead. Although the evaluation of a computer model is less predictable than measuring physical phenomena, our experiments suggest that despite of its simplified nature, the proposed model captures the general behavior of foliar BDF's and does not introduce significant errors along the rendering pipeline.

There are some practical issues that we intend to address to improve the results obtained so far. Since the rendering of organic materials like plants have a strong wavelength dependency, the quality of the images is directly affected by the spectral sampling. We plan to investigate methods for guiding the wavelength selection, for instance the strategy proposed by Meyer [24], to determine the group of wavelengths that fits best the perceptual and computational requirements of these applications. Future efforts will also include developing practical techniques to exploit the parallel implementation of the proposed model in shared memory multiprocessor workstations.

References

[1] W. Allen, A. Richardson, and J. Thomas. Iteraction of isotropic light with a compact plant leaf. *Journal of the Optical Society of America*, 59(10):1376–1379, 1969.

[2] G. V. G. Baranoski and J. G. Rokne. An algorithmic reflectance and transmittance model for plant tissue. *Computer Graphics Forum (EUROGRAPHICS Proceedings)*, 16(3):141–150, September 1997.

[3] T. Brakke, J. Smith, and J. Harnden. Bidirectional scattering of light from tree leaves. *Remote Sensing of Environment*, 29:175–183, 1989.

[4] H. Breece and R. Holmes. Bidirectional scattering characteristics of healthy green soybean and corn leaves in vivo. *Applied Optics*, 10(1):119–127, January 1971.

[5] H. Gausman and W. Allen. Optical parameters of leaves of 30 plant species. *Plant Physiology*, 52:57–62, 1973.

[6] A. Glassner. *Principles of Digital Image Synthesis*. Morgan Kaufmann, San Francisco, first edition, 1995.

[7] Y. M. Govaerts, S. J. amd M. Verstraete, and S. L. Ustin. Three-dimensional radiation transfer modeling in a dycotyledon leaf. *Applied Optics*, 35(33):6585–6598, November 1996.

[8] L. Grant. Diffuse and specular characteristics of leaf reflectance. *Remote Sensing of Environment*, 22:309–322, 1987.

[9] R. Hall. *Illumination and Color in Computer Generated Imagery*. Springer-Verlag, New York, 1989.

[10] R. A. Hall and D. P. Greenberg. A testbed for realistic image synthesis. *IEEE Computer Graphics and Applications*, 3(8):10–20, November 1983.

[11] J. Hammerley and D. Handscomb. *Monte Carlo Methods*. Wiley, New York, N.Y., 1964.

[12] P. Hanrahan and W. Krueger. Reflection from layered surfaces due to subsurface scattering. *Computer Graphics (SIGGRAPH Proceedings)*, pages 165–174, August 1993.

[13] S. Jacquemoud and F. Baret. Prospect: A model of leaf optical properties spectra. *Remote Sensing of Environment*, 34(2):75–92, 1990.

[14] J. Kajiya. The rendering equation. *Computer Graphics (SIGGRAPH Proceedings)*, 20(4):143–150, August 1986.

[15] Q. Kay, H. Daoud, and C. Stirton. Pigment distribution, light reflection and cell structure in petals. *Botanic Journal of the Linnean Society*, 83:57–84, 1981.

[16] E. Lafortune and Y. D. Willems. Using the modified phong reflectance model for physically based rendering. Technical report, Department of Computer Science, K.U. Leuven, November 1994.

[17] P. Lalonde and A. Fournier. A wavelet representation of reflectance functions. *IEEE Transaction on Visualization and Computer Graphics*, 3(4):329–336, October 1997.

[18] R. R. Lewis. Making shaders more physically plausible. In M. Cohen and C. Puech, editors, *Proc. of the Fourth Eurographics Rendering Workshop*, pages 47–62, June 1993.

[19] C. Lilley, F. Lin, W. Hewitt, and T. Howard. *Colour in Computer Graphics*. ITTI Computer graphics and Visualisation, Manchester Computing Centre, The University of Manchester, Manchester, England, December 1993.

[20] Q. Ma, A. Nishimura, P. Phu, and Y. Kuga. Transmission, reflection and depolarization of an optical wave for a single leaf. *IEEE Transactions on Geoscience and Remote Sensing*, 28(5):865–872, September 1990.

[21] D. L. MacAdam. *Color Measurements Theme and Variations*. Springer Verlag, Berlin, 1981.

[22] G. Martin, D. Myers, and T. Vogelmann. Characterization of plant epidermal lens effects by a surface replica technique. *Journal of Experimental Botany*, 42(238):581–587, May 1991.

[23] N. Max, C. Mobley, B. Keating, and E. Wu. Plane-parallel radiance transport for global illumination in vegetation. In J. Dorsey and P. Slusallek, editors, *Rendering Techniques'97 (Proceedings of the Eight Eurographics Rendering Workshop)*, pages 239–250. Springer-Verlag, June 1997.

[24] G. W. Meyer. Wavelength selection for synthetic image generation. *Computer Vision, Graphics, and Image Processing*, 41:57–79, 1988.

[25] C. Schlick. A survey of shading and reflectance models. *Computer Graphics Forum (EUROGRAPHICS Proceedings)*, 13(2):121–131, 1994.

[26] P. Shirley. *Physically based lighting for computer graphics*. PhD thesis, Dept. of Computer Science, University of Illinois, November 1990.

[27] L. Smail. *Analytic Geometry and Calculus*. Appleton-Century-Crofts, New York, 1953.

[28] C. J. Tucker and M. Garrat. Leaf optical system modeled as a stochastic process. *Applied Optics*, 16(3):635–642, 1977.

[29] T. Vogelmann and G. Martin. The functional significance of palisade tissue: penetration of directional versus diffuse light. *Plant, Cell and Environment*, 16:65–72, 1993.

[30] G. Ward. Measuring and modeling anisotropic reflection. *Computer Graphics (SIGGRAPH Proceedings)*, pages 265–272, July 1992.

[31] J. Woolley. Reflectance and transmittance of light by leaves. *Plant Physiology*, 47:656–662, 1971.